


RESEARCH ARTICLE

Reaction Engineering, Kinetics and Catalysis

An experimental/computational study of steric hindrance effects on CO₂ absorption in (non)aqueous amine solutionsQinlan Luo¹ | Rui Dong¹ | Bohak Yoon² | Hongxia Gao¹ | Mengjie Chen¹ | Gyeong S. Hwang² | Zhiwu Liang¹ ¹Joint International Center for CO₂ Capture and Storage (iCCS), Hunan Provincial Key Laboratory for Cost-Effective Utilization of Fossil Fuel Aimed at Reducing CO₂ Emissions, College of Chemistry and Chemical Engineering, Hunan University, Changsha, PR China²McKetta Department of Chemical Engineering, University of Texas at Austin, Austin, Texas, USA

Correspondence

Hongxia Gao and Zhiwu Liang, Joint International Center for CO₂ Capture and Storage (iCCS), Hunan Provincial Key Laboratory for Cost-Effective Utilization of Fossil Fuel Aimed at Reducing CO₂ Emissions, College of Chemistry and Chemical Engineering, Hunan University, Changsha 410082, PR China.
Email: hxgao@hnu.edu.cn and zwliang@hnu.edu.cn

Funding information

China Outstanding Engineer Training Plan for Students of Chemical Engineering & Technology in Hunan University, Grant/Award Number: MOE-No. 2011-40; Hunan Key R & D Program Project, Grant/Award Number: 2020NK2015; Korea CCS R&D Center (KCRC) grant, Grant/Award Number: 2017M1A8A1072016; National Key Research & Development Program - Intergovernmental International Science and Technology Innovation Cooperation Project, Grant/Award Number: 2021YFE0112800; National Natural Science Foundation of China, Grant/Award Numbers: 21878073, 21978075, 22078083, 22138002; R. A. Welch Foundation, Grant/Award Number: F-1535; science and technology innovation Program of Hunan Province, Grant/Award Number: 2020RC5032; Texas Advanced Computing Center (TACC) at the University of Texas at Austin, Grant/Award Number: OCI-1134872

Abstract

The reaction kinetics and molecular mechanisms of CO₂ absorption using nonaqueous and aqueous monoethanolamine (MEA)/methyldiethanolamine (MDEA)/2-amino-2-methy-1-propanol (AMP) solutions were analyzed by the stopped-flow technique and *ab initio* molecular dynamics (AIMD) simulations. Pseudo first-order rate constants (k_0) of reactions between CO₂ and amines were measured. A kinetic model was proposed to correlate the k_0 to the amine concentration, and was proved to perform well for predicting the relationship between k_0 and the amine concentration. The experimental results showed that AMP/MDEA only took part in the deprotonation of MEA-zwitterion in nonaqueous MEA + AMP/MEA + MDEA solutions. In aqueous solutions, AMP can also react with CO₂ through base-catalyzed hydration mechanism beside the zwitterion mechanism. Molecular mechanisms of CO₂ absorption were also explored by AIMD simulations coupled with metadynamics sampling. The predicted free-energy barriers of key elementary reactions verified the kinetic model and demonstrated the different molecular mechanisms for the reaction between CO₂ and AMP.

KEYWORDS

ab initio molecular dynamics, CO₂ absorption mechanism, kinetic model, reaction kinetics, steric hindrance

1 | INTRODUCTION

Massive emission of carbon dioxide (CO₂) from the combustion of fossil fuels, like coal, oil, and natural gas, leads to global warming and many serious environmental problems.^{1,2} From 1958 to 2010, the CO₂

concentration in the atmosphere increased from 315 to 390 ppm,³ and the global temperature is expected to increase by 3°C by the end of the century, if there is no significant reduction of CO₂ emissions.⁴ Therefore, aggressive action is needed to reduce CO₂ emissions, which is the common responsibility of all countries in the world. Among various CO₂ capture methods, including chemical looping, adsorption, physical absorption, chemical absorption, membrane absorption, cryogenic distillation, and gas

Qinlan Luo, Rui Dong, and Bohak Yoon contributed equally to this work.

hydrates,^{2,5,6} chemical absorption is one of the most widely implemented technologies.⁷ It has the advantages of the fast absorption rate and high adaptability for CO₂ capture from highly diluted gas, which can be applied to the existing thermal power plants with minimal process modification.⁸

In the last several years, using amine solutions for the chemical absorption of CO₂ has been an efficient and promising way in the CO₂ capture area,⁹ which has timeliness, high removal rate, and high purity for the reduction of CO₂ emission from conventional thermal power plants.¹⁰ A good number of amine-based solutions have been proposed by researchers,^{11,12} but all solutions have pros and cons. Therefore, the development of amine blends attracts more attention, as it can combine the advantages of different kinds of amines, such as obtaining high absorption rate, high CO₂ loading, low heat of reaction, low energy consumption of desorption, and low corrosion rate.^{1,13} While most of the studies only focus on the absorption or desorption performance of amine blends through experimental investigation,¹⁴ the fundamental mechanisms underlying the CO₂ absorption or desorption in amine blends are still unclear, which plays a significant and directive role in the development of new amine blends.

Several studies^{15,16} have pointed out that the use of sterically hindered amines is a suitable choice for the postcombustion CO₂ capture, which have certain positive characteristics upon both the absorption process and desorption process owing to their special molecular structures. Despite the widely accepted zwitterion mechanism¹⁷ for primary and secondary amines and the base-catalyzed hydration mechanism for tertiary amines,¹⁸ the underlying mechanism of CO₂ absorption by 2-amino-2-methyl-1-propanol (AMP) remains highly debatable. On the basis of its high absorption rate and the bicarbonate as the primary products, Alper¹⁹ and Yin et al.²⁰ have speculated that CO₂ may first react with AMP to form the carbamate ion (AMPCOO⁻), and there after the unstable carbamate ion may undergo hydrolysis to form bicarbonate. On the contrary, some studies^{21,22} have demonstrated that the activation barrier for the hydrolysis of AMPCOO⁻ is high and also comparable to that for the hydrolysis of MEACOO⁻, implying that AMPCOO⁻ is as stable as MEACOO⁻ and may not easily undergo the hydrolysis to form bicarbonate.

Comparing to aqueous amine solutions, nonaqueous solutions have a significant advantage of low energy consumption for regeneration due to the low heat capacity and the negligible heat of vaporization,²³ with other advantages of less corrosiveness and low degradation.²⁴ Therefore, the nonaqueous amines solutions have risen in recent years as one of the most viable alternatives to the aqueous solutions,²⁵ and the reaction kinetics and mechanisms of CO₂ absorption in nonaqueous amines solutions are also worth to be discussed.

Several experimental instruments can be used for the kinetics analysis of the CO₂ absorption in amine solutions, such as the stirred cell reactor,²⁶ the wetted wall column,⁸ the bubbling reactor,²⁷ and the stopped-flow apparatus.²⁸ Among them, the stopped-flow technique²⁹ shows the advantages of high sensitivity, high reliability, easy and fast operation, less consumption of solutions, and economical efficiency. Thus, it is widely used for the kinetics investigations of the reactions between dissolved CO₂ and kinds of amine solutions or blends.

Numbers of kinetic studies for reactions between CO₂ and sterically hindered amines in both nonaqueous and aqueous solutions have been performed using the stopped-flow technique. While most of them only focus on the absorption performance of different hindered amines,³⁰ the kinetic model of the rate constants to predict reactions rates of amines,³¹ or the qualitative effects of steric hindrance on the reaction rate still remains unclear.³²

In addition, several studies have also been conducted in our group, in which Liu and Luo et al.³³ have observed that the base-catalyzed hydration mechanism is precise in predicting the CO₂ absorption rates in hindered amines (2-(isopropylamino)ethanol (IPAE) and 2-[(1,1-dimethylethyl)amino]ethanol (TBAE)) solutions. Liu and Ling et al.³⁴ have explored the effects of steric hindrance on CO₂ absorption performance, the steric hindrance effect of the position of the alkyl group on second-order reaction rate and solubility, and the Brønsted correlation of second-order reaction rate and pK_a values for sterically hindered alkanolamines (2-methyl-ethanolamine (MAE), 2-ethyl-ethanolamine (EAE), 1-amino-2-propanol (1-AP), 2-amino-1-propanol (2-AP), 3-amino-1-propanol (3-AP), and AMP). However, the reaction kinetics and fundamental mechanism of CO₂ absorption in nonaqueous and aqueous sterically hindered amines solutions, as well as the key reason for their difference, are still unclear to this point. Bougie and Iliuta³⁵ also have suggested that new kinetic studies for all sterically hindered amines, even for AMP, would be very welcome, based on their comprehensive review on different aspects concerning several binary and multicomponent systems of CO₂-sterically hindered amine-based absorbents.

In the present study, we probe CO₂ absorption reaction with amines in nonaqueous/aqueous solutions, excepting that the reaction mechanisms of sterically hindered amine (AMP) can be verified in both nonaqueous and aqueous solutions, compared to that of primary amine (monoethanolamine (MEA)) and tertiary amine (methyldiethanolamine (MDEA)). The stopped-flow apparatus was implemented to analyze the reaction kinetics and explore the reaction model of CO₂ reacting with AMP in aqueous and nonaqueous solutions. *Ab initio* molecular dynamics (AIMD) simulations coupled with metadynamics sampling were also conducted to examine whether the mechanism and kinetics of CO₂ capture by AMP would be affected by the solvation environment, as compared to the experimental results.

2 | EXPERIMENTS AND SIMULATIONS

2.1 | Experimental section

The stopped-flow apparatus, model SF-61DX manufactures by Hi-Tech Scientific, Ltd. (U.K.), was used to explore the reaction kinetics of CO₂ absorption in nonaqueous/aqueous amine solutions, as shown in Figure 1. The stopped-flow apparatus contains four main sections: a sample handling unit, an electrical conductivity detector, a A/D converter, and a microprocessor. Prior to the experiments, two seal syringes were preheated to a target temperature by the water bath thermostat, filled with amine solution and CO₂ solution, respectively.

Then, both amine solution and CO₂ solution were pumped into the reaction cell and stopped instantly by the stop syringes to achieve the homogeneity. At the same time, the electrical conductivity of the mixed solution was measured and plotted as time according to the equation of $Y = -A \cdot \exp(-k_0 \cdot t) + C$, and the pseudo-first-order reaction rate constant (k_0) were calculated. Other details of the experimental system and experimental procedure can be found in our previous studies.^{7,9,36}

In this way, the k_0 for the reaction of CO₂ and MEA, AMP, MDEA, MEA + AMP, MEA + MDEA in nonaqueous and aqueous systems were estimated as a function of amine concentration. In the nonaqueous system, the ethanol was selected as the solvent, and the water was the solvent in the aqueous system. The details of all the nonaqueous and aqueous systems, explored in this study, were shown in the Table 1. The

rate constant of each system was estimated at least four times and averaged to estimate the reliability and reproducibility.

Before the formal experiments, the k_0 for the reaction between CO₂ and aqueous MEA solutions with different MEA concentrations at 303 K was measured. The estimated k_0 were compared to previously published data and showed a good agreement with the Ali's results published in the literature³⁷, as shown in Figure 2.

2.2 | Simulation section

Ab initio molecular dynamics simulations (AIMD) based on density functional theory (DFT) were performed with the Car-Parrinello molecular dynamics (CPMD) code. Metadynamics (MTD) sampling for the reconstruction of the free-energy (FE) profile was employed via PLUMED plugin. The generalized gradient approximation exchange-correlation functional revised by Perdew, Burke, and Ernzerhof (revPBE³⁸) was used; the choice of revPBE functional was discussed in literatures^{39, 40}. The kinetic energy cutoff for the plane wave

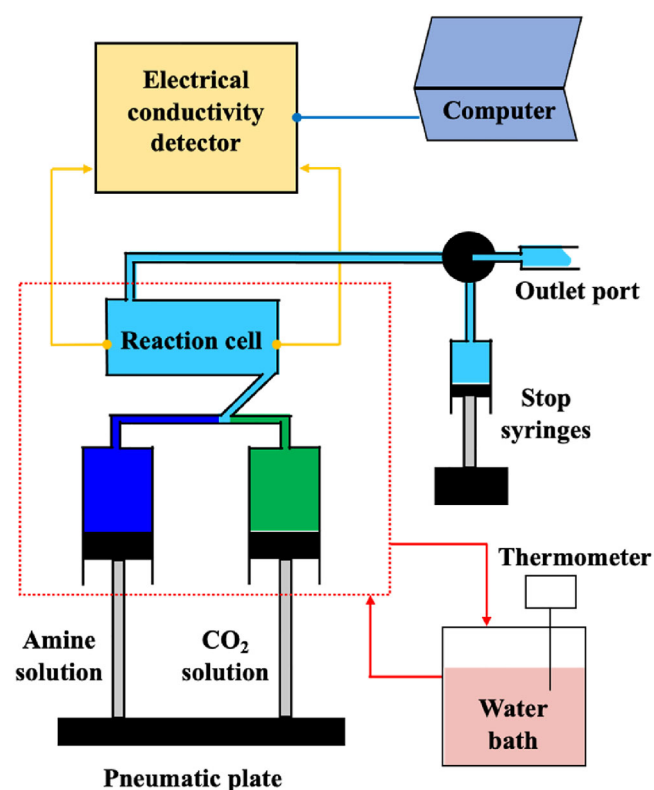


FIGURE 1 Schematic diagram of the stopped-flow apparatus

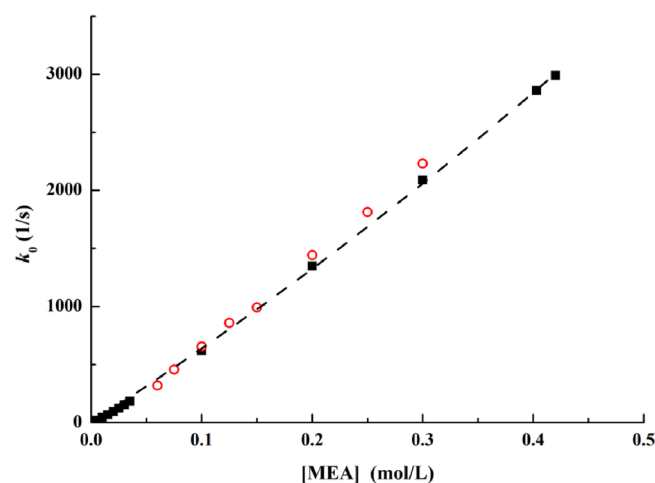


FIGURE 2 Comparison of the pseudo-first-order rate constants (k_0) for the reaction between CO₂ and MEA aqueous solutions between this study and that in the literature at 303.15 K with the MEA concentration range of 0.06–0.3 mol/L. (red open circle symbol: present study, black dashed line with solid square symbols: Ali's results)

TABLE 1 Details of the nonaqueous and aqueous solutions explored in this study

Solution	Solute A	Concentration of Solute A, mol/L	Solute B	Concentration of Solute B, mol/L	Solvent
Nonaqueous MEA solutions	MEA	0.1–0.5	—	—	Ethanol
Nonaqueous AMP solutions	AMP	0.4–0.6	—	—	Ethanol
Nonaqueous MEA + AMP solutions	MEA	0.1–0.4	AMP	0.1–0.6	Ethanol
Nonaqueous MEA + MDEA solutions	MEA	0.1–0.4	MDEA	0.1–0.6	Ethanol
Aqueous MEA solutions	MEA	0.1–0.4	—	—	Water
Aqueous AMP solutions	AMP	0.1–0.5	—	—	Water
Aqueous MDEA solutions	MDEA	0.1–0.6	—	—	Water

basis was 40 Rydberg. The timestep was set to 7 a.u. (0.17 fs), and fictitious electrons' mass was equal to 700 a.u. The Nosé–Hoover chain thermostat was used to control the temperature (313 K) under the NVT ensemble. The frequency for the ionic thermostat and the electron thermostat was set to 3000 and 10,000 cm^{-1} , respectively.

The MTD technique can be implemented in conjunction with CPMD to accelerate the dynamics,⁴¹ as CPMD simulation is computationally too expensive to simulate for experimental timescales. In metadynamics, a biased potential of the Gaussian-like hill is deposited at small time intervals in the coordinate space of interest to fill up the FE surface. The accumulation of these potential hills can construct the FE surface with respect to the chosen collective variables. The potential hills were collected every 100 timesteps (1 timestep = 0.17 fs) over a trajectory of about 100 ps. Other details of our simulations can be found in the literatures ^{39, 40, 42, 43}.

3 | REACTION MECHANISMS AND KINETIC MODELS

For the CO_2 absorption in primary or secondary amine solutions, the zwitterion mechanism is widely appreciated by researchers, indicating that in the aqueous solutions following carbon-nitrogen bond formation (Reaction (1)) the amine proton is transferred to a basic molecule (Reaction (2)) yielding charged products. Caplow's results¹⁷ also have pointed out that the rate limiting step of CO_2 absorption in the weakly basic amine and basic amines is the carbon-nitrogen bond formation and proton transfer. The termolecular mechanism⁴⁴ can also be used to explain the reactions between CO_2 and primary or secondary amine (Reaction (3)). Meanwhile, the base-catalyzed hydration mechanism⁴⁵ can be used to describe the reaction between CO_2 and tertiary amines, in which tertiary amines react with H_2O and CO_2 simultaneously or appear to act only as a weak base to produce free OH^- to react with CO_2 to form bicarbonate (Reaction (4)).



The reaction mechanism for the CO_2 absorption in sterically hindered amines solutions appears to be more complex, as the reaction product is bicarbonate rather than the alkylammonium carbamate formed in primary or secondary amine solutions; the reaction rate is much faster than that in the tertiary amines solutions.

According to the zwitterion mechanism, the overall reaction rate can be derived based on the quasi-steady-state condition,^{11,28} which

assumes that the concentration of the intermediate zwitterion is zero, as shown in Equation (5). And, the reaction rate can be showed in the format of Equation (7), as the order of the reaction with respect to the CO_2 is one, which has been confirmed by several researchers.^{46,47}

$$r_{\text{CO}_2} = \frac{[\text{CO}_2][\text{Amine}]}{(1/k_2) + (k_{-1}/k_2 \sum k_{\text{Base}}[\text{B}])} = \frac{[\text{CO}_2][\text{Amine}]}{(1/k_2) + (1/\sum k_{\text{B}}[\text{B}])} \quad (5)$$

$$k_{\text{B}} = \frac{k_2 k_{\text{Base}}}{k_{-1}} \quad (6)$$

$$r_{\text{CO}_2} = k_0 [\text{CO}_2] \quad (7)$$

$$k_0 = \frac{[\text{Amine}]}{(1/k_2) + (1/\sum k_{\text{B}}[\text{B}])} \quad (8)$$

For the Equation (8), there are two limiting cases: (a) when the $1/k_2$ is much bigger than the $1/\sum k_{\text{B}}[\text{B}]$, the deprotonation of zwitterion is much faster than the reversion reaction rate of zwitterion formation, while k_0 can be expressed in the Equation (9), and (b) when the $1/k_2$ is much smaller than the $1/\sum k_{\text{B}}[\text{B}]$, the deprotonation of zwitterion becomes the rate-determining step as its reaction rate is slower than the reverse reaction rate of zwitterion formation, while k_0 can be reduced to Equation (10).

$$k_0 = k_2 [\text{Amine}] \quad (9)$$

$$k_0 = \left(\sum k_{\text{B}}[\text{B}] \right) [\text{Amine}] \quad (10)$$

By measuring the k_0 of amine solutions with different amine concentrations, the order of the reaction can be estimated by fitting the k_0 to the amine concentration with the power-law Equation (11).

$$k_0 = k_n [\text{Amine}]^n \quad (11)$$

Our initial experimental results point out that the reaction order of CO_2 absorption in nonaqueous MEA solution and aqueous MEA solution is 1.89 and 1.19, respectively, which indicate that the Equation (9) is not suitable to describe the reaction between CO_2 and MEA in both nonaqueous and aqueous system. Considering that the concentration ratio of amine and CO_2 ($[\text{Amine}]/[\text{CO}_2]$) was kept at the value of 20 in all experiments, we could neglect the reverse reaction of zwitterion formation, and zwitterion deprotonation.

Therefore, based on the zwitterion mechanism and base-catalyzed hydration mechanism, we attempt to propose the hypothetical kinetic model for reactions between CO_2 and MEA, AMP, MDEA, MEA + AMP, MEA + MDEA in both nonaqueous and aqueous systems. If the hypothetical kinetic model can describe our experiments and simulation results, our intrinsic kinetic model based on the fundamental mechanisms of CO_2 absorption in nonaqueous and aqueous systems can be confirmed suitable. The hypothetical kinetic model is as follows:

In the nonaqueous MEA solution, both MEA and ethanol can play a significant role in the deprotonation of MEA-zwitterion; thus the derivation of k_0 can be expressed in Equation (12).

$$k_0 = k_{2,MEA,non}[MEA]k_{MEA-MEA,non}[MEA] + k_{2,MEA,non}[MEA]k_{MEA-Eth,non}[ETHANOL] = K_{MEA-MEA,non}^Z[MEA][MEA] + K_{MEA-Eth,non}^Z[MEA] \quad (12)$$

As pointed out in references 44, 48, the reaction between CO₂ and MDEA may not likely occur without the existence of water. Thus MDEA only plays a role of proton acceptor after the formation of MEA-zwitterion in nonaqueous MEA+MDEA solutions during CO₂ absorption. Thereafter, the k_0 can be expressed in the following equations:

$$k_0 = K_{MEA-MDEA,non}^Z[MEA][MDEA] + K_{MEA-MEA,non}^Z[MEA][MEA] + K_{MEA-Eth,non}^Z[MEA] \quad (13)$$

$$k_0 = A[MDEA] + B \quad (14)$$

$$A = K_{MEA-MDEA,non}^Z[MEA] \quad (15)$$

$$B = K_{MEA-MEA,non}^Z[MEA][MEA] + K_{MEA-Eth,non}^Z[MEA] \quad (16)$$

$$k_0 = C[MEA][MEA] + D[MEA] \quad (17)$$

$$C = K_{MEA-MEA,non}^Z \quad (18)$$

$$D = K_{MEA-MDEA,non}^Z[MDEA] + K_{MEA-Eth,non}^Z \quad (19)$$

We can then compare the change tendency of k_0 values with the change of AMP concentration in nonaqueous AMP/MEA + AMP solutions with that of nonaqueous MEA solutions and nonaqueous MEA + MDEA solutions, to find out the role of AMP in the CO₂ absorption.

Extending to the reaction kinetics to the aqueous solutions, k_0 of reaction between CO₂ and MEA can be explained in the following equation.

$$k_0 = k_{2,MEA,aq}[MEA]k_{MEA-MEA,aq}[MEA] + k_{2,MEA,aq}[MEA]k_{MEA-H_2O,aq}[H_2O] = K_{MEA-MEA,aq}^Z[MEA][MEA] + K_{MEA-H_2O,aq}^Z[MEA] \quad (20)$$

For aqueous MDEA solutions, the k_0 can be obtained by the following expression:

$$k_0 = k_{3,MDEA,aq}[MDEA][H_2O] = K_{MDEA,aq}^C[MDEA] \quad (21)$$

Similarly, by comparing the reaction kinetics of the CO₂ absorption in aqueous AMP solutions to that in aqueous MEA solutions and that in aqueous MDEA solutions, a kinetic model can be obtained for the aqueous AMP system.

If the observed k_0 of the reaction between CO₂ and nonaqueous MEA, MEA + AMP, and MEA + MDEA solutions with different MEA, AMP, and MDEA concentration, can be well described by the above model, we may elucidate fundamental mechanisms of CO₂ absorption in nonaqueous and aqueous amine solutions, especially for the AMP case.

4 | RESULTS AND DISCUSSION

As aforementioned, water plays a significant role in the reactions between sterically hindered amines and CO₂. To explore the reaction mechanisms underlying CO₂ capture by AMP solutions, with an emphasis on the important effects of water molecules, the kinetics of CO₂ absorption into aqueous AMP or nonaqueous MEA + AMP were investigated by using the stopped-flow apparatus. We also compared our results to that of aqueous MEA, aqueous MDEA, nonaqueous MEA, or nonaqueous MEA + AMP as reference.

First, we attempted to measure the k_0 values of reactions between MEA, AMP, MDEA, and CO₂ in nonaqueous MEA, AMP, and MDEA solutions with different MEA, AMP, and MDEA concentrations using stopped-flow apparatus. Only the k_0 of the reactions between MEA and CO₂ in nonaqueous MEA solutions and the nonaqueous AMP solutions with high AMP concentration ([AMP] ≥ 0.4 mol/L) can be measured, indicating the low reaction rate between CO₂ and nonaqueous AMP solutions with the low AMP concentration ([AMP] < 0.4 mol/L). The phenomenon also implies that the reactions between MDEA and CO₂ in nonaqueous MDEA solutions can be negligible, which consistent with the experimental results observed by Versteeg and van Swaaij.⁴⁹

Considering the low reaction rate underlying CO₂ absorption in nonaqueous AMP solutions and negligible reaction between CO₂ and nonaqueous MDEA solutions, we mixed MEA with AMP and MDEA in ethanol to form nonaqueous MEA + AMP and MEA + MDEA solutions to further explore the reaction mechanisms among MEA, AMP, MDEA, and CO₂ without the participation of water. Then, we can infer the fundamental mechanism of the reaction between CO₂ and AMP in nonaqueous systems by comparing the kinetic behavior of CO₂ absorption in nonaqueous MEA + AMP and MEA + MDEA solutions. The reaction kinetics of CO₂ absorption in nonaqueous MEA, nonaqueous MEA + AMP, and nonaqueous MEA + MDEA solutions were determined with the MEA concentration range of 0.1–0.4 mol/L and both AMP and MDEA concentration range of 0.05–0.6 mol/L at 298.15 K. The measured k_0 of nonaqueous MEA + AMP solutions and nonaqueous MEA + MDEA solutions are shown in Figure 3, with the increase of AMP concentration and MDEA concentration, respectively. Compared to the nonaqueous MEA + AMP solutions, the aqueous MEA + MDEA solutions have low k_0 values and CO₂ absorption rates, due to the fact that pK_a of MDEA (pK_a = 8.76, 293 K) is lower than that of AMP (pK_a = 9.88, 293 K).⁵⁰ It is worth noting that pK_a is one of the key factors determining the role of proton acceptor during the proton abstraction process.

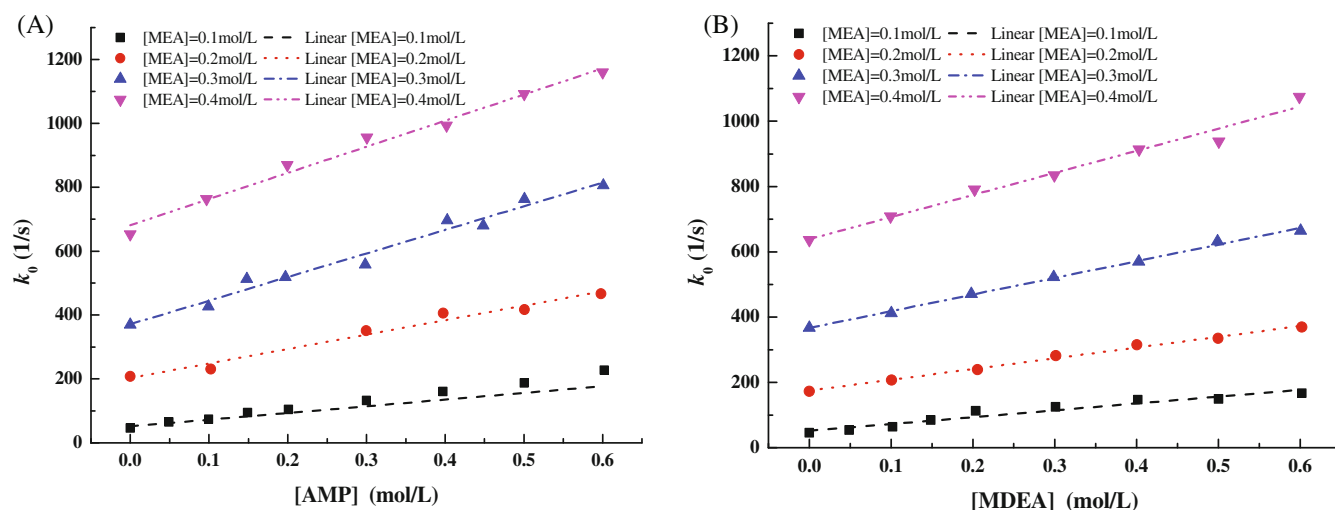


FIGURE 3 The k_0 values of the reactions between CO_2 and nonaqueous MEA + AMP solutions (A), or between CO_2 and nonaqueous MEA + MDEA solutions (B), as a function of AMP concentration (A) or MDEA concentration (B), respectively

TABLE 2 Parameters of linear fitting (as shown in Equations (13–15)), relating the k_0 values of nonaqueous MEA + AMP or MEA + MDEA solutions to the AMP or MDEA concentration

Nonaqueous solutions	[MEA] mol/L	A 1/s/(mol/L)	B 1/s	$K_{\text{MEA-AMP,non}}^Z / K_{\text{MEA-MDEA,non}}^Z$ 1/s/(mol/L) ²	$K_{\text{MEA-MEA,non}}^Z$ 1/s/(mol/L) ²	$K_{\text{MEA-Eth,non}}^Z$ 1/s/(mol/L)
MEA + AMP	0.1	289.54	47.521	2228	3837.7	152.04
	0.2	452.16	203.24			
	0.3	738.97	371.3			
	0.4	818.31	681.48			
MEA + MDEA	0.1	209.6	49.832	1701.5	3646.8	136.47
	0.2	329.39	174.94			
	0.3	509.92	367.07			
	0.4	676.78	638.82			
MEA	0.1–0.5				3725.3	145.65

From our results, the increase of the MEA, AMP, MDEA concentration ([MEA], [AMP], and [MDEA]) leads to the increase of k_0 value in both nonaqueous MEA + MDEA and nonaqueous MEA + AMP systems, suggesting that MEA, AMP, and MDEA all play positive roles in CO_2 absorption. At a certain MEA concentration, the k_0 value of nonaqueous MEA + AMP and MEA + MDEA solutions was remarkably correlated linearly with the AMP concentration ([AMP]) and MDEA concentration ([MDEA]), respectively, which is consistent with the relationship between k_0 value and [AMP]/[MDEA], as shown in Equation (13). Based on the linear relationship, the parameter A and B in Equation (14) can be calculated, as shown in Table 2, which showed a good linear correlation and a second-order polynomial correlation with the MEA concentration ([MEA]), respectively, as shown in Figure 4. Thereafter, the second reaction constants ($K_{\text{MEA-MEA,non}}^Z$, $K_{\text{MEA-AMP,non}}^Z$, and $K_{\text{MEA-MDEA,non}}^Z$) can be obtained, based on the two-step reaction mechanism. The relative difference among the reaction constants can determine which molecule

plays a role of proton acceptor in the second step (deprotonation of MEA-zwitterion).

The calculated values of $K_{\text{MEA-MEA,non}}^Z$ from nonaqueous MEA + AMP, nonaqueous MEA + MDEA, and nonaqueous MEA were very close, suggesting that our hypothesis model (Equations (12) and (13)) can very well describe the corresponding systems. The relation of second reaction constants is $K_{\text{MEA-MEA,non}}^Z > K_{\text{MEA-AMP,non}}^Z > K_{\text{MEA-MDEA,non}}^Z$, indicating that the proton transfer from MEA-zwitterion to MEA is the fastest and that from MEA-zwitterion to MDEA is the slowest. This phenomenon also shows that the deprotonation of MEA-zwitterion in nonaqueous solution may not be purely determined by pK_a ($\text{pK}_a(\text{AMP}) > \text{pK}_a(\text{MEA}) > \text{pK}_a(\text{MDEA})$). As the rearrangement of ethanol molecules are much slower than that of water molecules, the proton transfer is also closely related to molecular size, molecular structure and steric hindrance effect of amines. The reaction constant of the proton transfer with through ethanol molecule ($K_{\text{MEA-Eth,non}}^Z$) calculated from nonaqueous MEA, nonaqueous

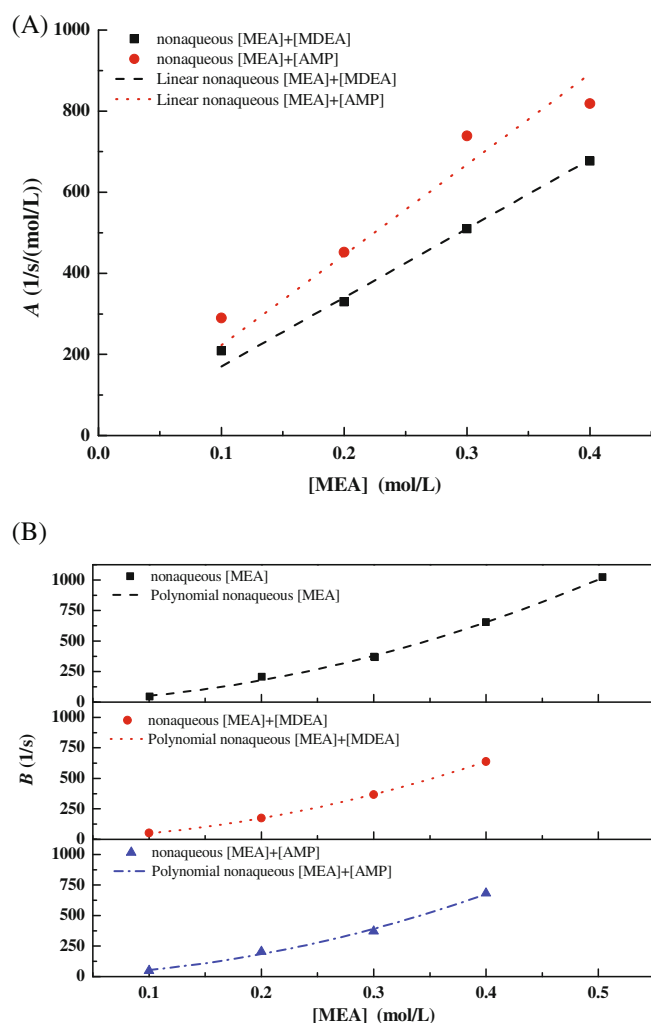


FIGURE 4 The values of parameter A and parameter B in Equation (14) show the linear relationship (A) and the 2-order polynomial relationship (B) with the MEA concentration, respectively

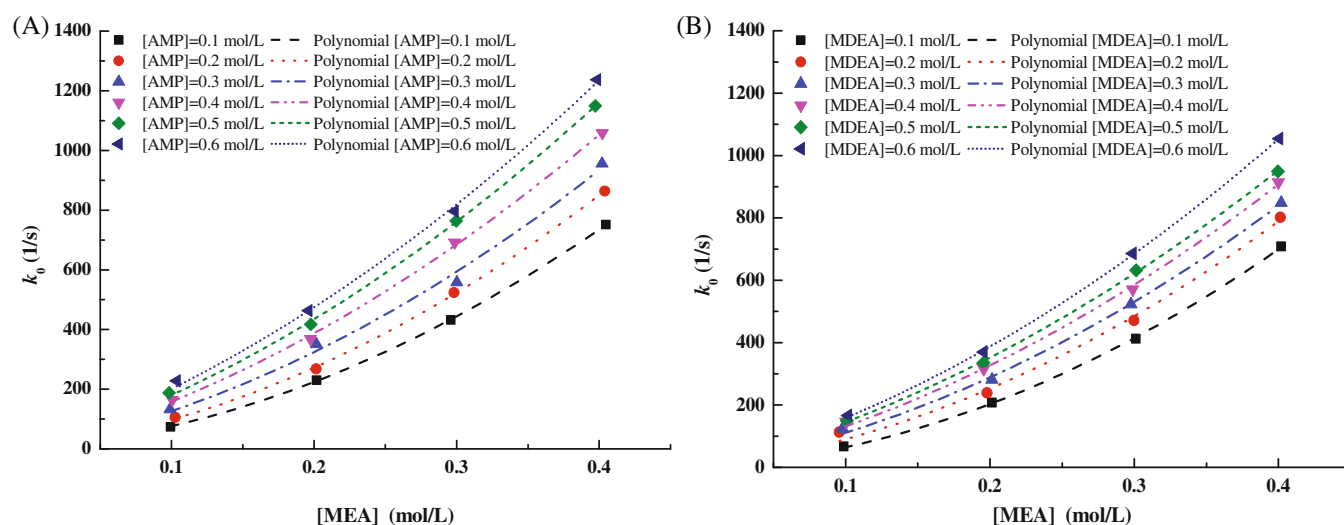


FIGURE 5 The k_0 values of the reactions between CO_2 and nonaqueous MEA + AMP solutions (A), or between CO_2 and nonaqueous MEA + MDEA solutions (B), as a function of the MEA concentration

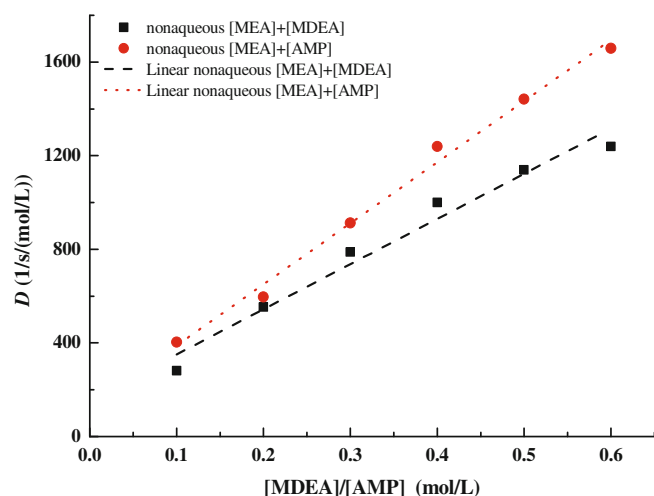
MEA + AMP, and nonaqueous MEA + MDEA also showed similar results (from 136.47 to 152.04 $\text{s}^{-1} \cdot (\text{mol/L})^{-1}$), demonstrating that the deprotonation of MEA-zwitterion with the help of ethanol molecule may occur in all nonaqueous solutions, despite that the reaction rate was much slower than that by MEA, AMP, and MDEA.

To further validate the reliability and the accuracy of our hypothesis model, the relationship between k_0 and the MEA concentration in nonaqueous MEA + AMP or nonaqueous MEA + MDEA was also explored, as shown in Figure 5. This figure shows that both the AMP and MDEA concentration had positive effects on the CO_2 absorption rate. It can be easily found out that, in all nonaqueous MEA + AMP and nonaqueous MEA + MDEA solutions, the k_0 value of the reaction between CO_2 and amines has the polynomial correlation with the MEA concentration and well-fitted the Equation (17). The corresponding polynomial fitting coefficients C and D are shown in Table 3; thereafter, the value of $K_{\text{MEA-MEA,non}}^Z$ can be calculated from averaging the values of C. As shown in Figure 6, there exists a linear correlation between D and the AMP/MDEA concentration, which is consistent with that in Equation (19). Then, the slope and the intercept of the linear fitting equation can be assigned to $K_{\text{MEA-AMP,non}}^Z/K_{\text{MEA-MDEA,non}}^Z$ and $K_{\text{MEA-Eth,non}}^Z$, respectively.

The rank of estimated reaction constants is as follows: $K_{\text{MEA-MEA,non}}^Z > K_{\text{MEA-AMP,non}}^Z > K_{\text{MEA-MDEA,non}}^Z > K_{\text{MEA-Eth,non}}^Z$, which is consistent with that estimated from linear fitting in Table 2, indicating that the proton transfer from MEA-zwitterion to MEA is the fastest, and the proton transfer through ethanol is the slowest. The difference ratio of $K_{\text{MEA-AMP,non}}^Z$ and $K_{\text{MEA-MDEA,non}}^Z$, compared to that calculated from Linear fitting, was 13.46% and 17.17%, respectively. Moreover, the standard deviation of $K_{\text{MEA-MEA,non}}^Z$ and $K_{\text{MEA-Eth,non}}^Z$, estimated from linear fitting and second-order polynomial fitting in nonaqueous MEA, MEA + AMP, MEA + MDEA solutions, were 170.71 1/s/(mol/L)² and 11.14 1/s/(mol/L), respectively. These small differences demonstrate that our hypothetical kinetic model is a suitable intrinsic

TABLE 3 Parameters of second-order polynomial fitting (as shown in Equations (17–19)), relating the k_0 values of the nonaqueous MEA + AMP or MEA + MDEA solutions to the AMP or MDEA concentration

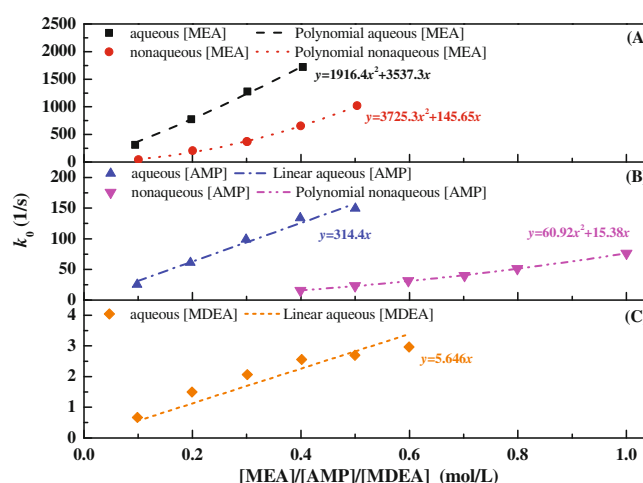
Nonaqueous solutions	[AMP]/[MDEA] mol/L	C 1/s/(mol/L) ²	D 1/s/(mol/L)	$K_{\text{MEA-AMP,non}}^Z/K_{\text{MEA-MDEA,non}}^Z$ 1/s/(mol/L) ²	$K_{\text{MEA-MEA,non}}^Z$ 1/s/(mol/L) ²	$K_{\text{MEA-Eth,non}}^Z$ 1/s/(mol/L)
MEA + AMP	0.1	3589.3	403.67	2610.5	3613.07	128.2
	0.2	3826.6	596.04			
	0.3	3557	912.14			
	0.4	3480.2	1239.7			
	0.5	3653.5	1441.4			
	0.6	3571.8	1658.3			
MEA + MDEA	0.1	3670.1	281.67	1930.5	3376.68	157.92
	0.2	3547.9	553.44			
	0.3	3274.5	778.22			
	0.4	3172.6	999.85			
	0.5	3109.4	1139.1			
	0.6	3485.6	1239.3			
MEA	0	3725.3	145.65		3725.3	145.65

**FIGURE 6** The values of parameter D in Equation (19) show the linear relationship with the AMP or MDEA concentration

kinetic model, which can describe the correlation between amine concentrations and pseudo-first-order reaction rate.

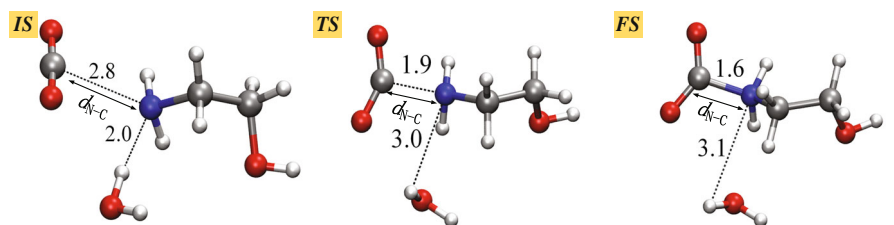
Based on the above experimental results, in nonaqueous MEA + AMP and MEA + MDEA solutions, AMP showed similar behavior with MDEA but showed certain differences when compared with that of MEA. AMP or MDEA only served as a proton acceptor, accelerating the deprotonation of MEA-zwitterion, but MEA can take part in both zwitterion formation and zwitterion deprotonation process. Meanwhile, AMP showed a better acceleration effect than MDEA, as can be expected from its high basicity.

But when we move to the pure nonaqueous amine solutions, reactions between CO₂ and AMP can be found in nonaqueous systems, suggesting that AMP can react with CO₂ in the reaction

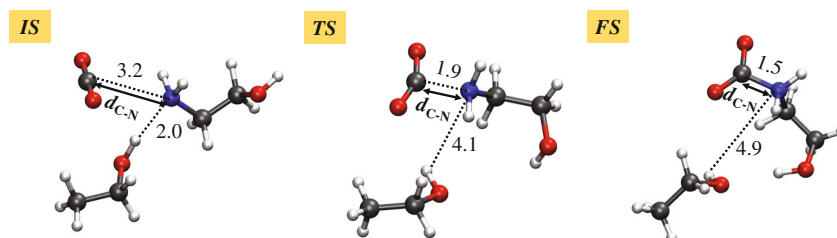
**FIGURE 7** The k_0 values of the reactions between CO₂ and nonaqueous/aqueous MEA solutions (A), between CO₂ and aqueous/nonaqueous AMP solutions (B), or between CO₂ and aqueous MDEA solution, as a function of MEA concentration (A), AMP concentration (B) or MDEA concentration (C), respectively

pathway of zwitterion formation and deprotonation, unlike MDEA in nonaqueous systems. Compared to the reaction rate in nonaqueous MEA solutions, the k_0 in nonaqueous AMP solutions is much smaller, as shown in Figure 7. Meanwhile, it can be found that values of both $K_{\text{AMP-AMP,non}}^Z$ (60.92 1/s/(mol/L)²) and $K_{\text{AMP-Eth,non}}^Z$ (15.38 1/s/(mol/L)), estimated from our hypothetical kinetic model, were much smaller than the values of $K_{\text{MEA-MEA,non}}^Z$ (3725.3 1/s/(mol/L)²) and $K_{\text{MEA-Eth,non}}^Z$ (145.65 1/s/(mol/L)), demonstrating that both AMP-zwitterion formation process and AMP-zwitterion deprotonation process were much slower than the MEA-zwitterion formation process and MEA-zwitterion deprotonation process. Therefore, in the

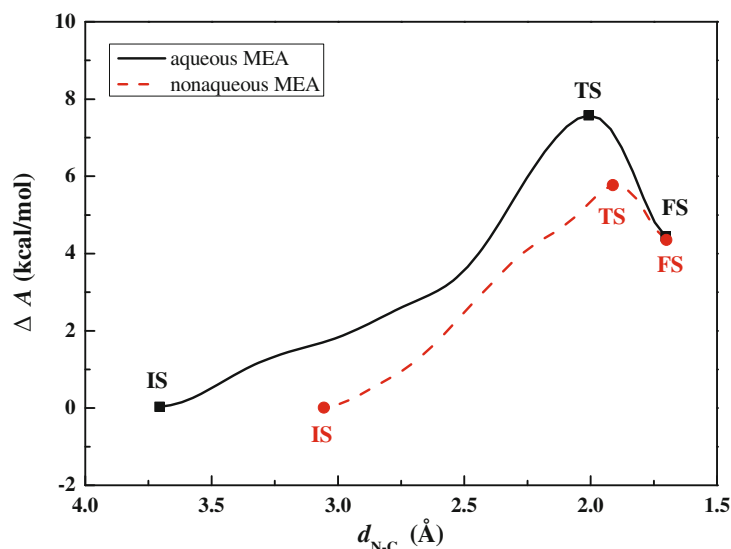
FIGURE 8 Free-energy profile for MEA-zwitterion formation in aqueous and nonaqueous MEA solution (C), that is, $\text{MEA} + \text{CO}_2 \rightarrow \text{MEA}^+\text{COO}^-$, predicted from metadynamics-biased Car–Parrinello MD simulation at 313 K. The collective variable employed is the distance between the C atom of CO_2 and the N atom of MEA ($d_{\text{N-C}}$). The structures and positions of the initial (IS), transition (TS), and final (FS) states in aqueous MEA solution (A) and nonaqueous MEA solution (B) are also indicated with the distance unit of Angstrom, where the blue, gray, red and white balls represent the N, C, O, and H atoms, respectively



(A) Structures of the initial (IS), transition (TS), and final (FS) states in aqueous MEA solution



(B) Structures of the initial (IS), transition (TS), and final (FS) states in nonaqueous MEA solution



(C) Free energy profiles for the reaction of zwitterion formation

nonaqueous MEA + AMP solutions, the MEA-zwitterion formation is much more favorable, and AMP may only play a positive role in the MEA-zwitterion deprotonation process.

To determine whether the key elementary reactions between AMP and CO_2 in aqueous solutions is the deprotonation of zwitterion after the zwitterion formation or the base-catalyzed hydration reaction, the reaction kinetics of CO_2 capture in aqueous MEA, AMP, MDEA solutions was also investigated by stopped-flow analysis.

The comparison between $K_{\text{MEA-MEA,non}}^Z$ of nonaqueous MEA solutions and $K_{\text{MEA-MEA,aq}}^Z$ of aqueous MEA solutions showed that the reaction of MEA-zwitterion formation in nonaqueous systems is faster. This can be explained by the strong hydrogen bonding in aqueous systems, which hinder the approach of CO_2 to MEA. Moreover, the proton transfer to water molecule dominates the MEA-zwitterion deprotonation in aqueous systems, while in

nonaqueous systems the proton transfer to MEA plays a leading role.

The relationship of the AMP concentration to k_0 value in aqueous AMP solutions can only be described by the linear correlation, in accordance with that in aqueous MDEA solutions. The results indicated the reaction order of one with respect to the amine, which agreed well with the results of Camacho et al.⁴⁷ As mentioned earlier, the k_0 of reaction between CO_2 and AMP in nonaqueous systems was predicted with second-order polynomial fitting of the AMP concentration. This demonstrates that the reaction between CO_2 and AMP can occur through both the zwitterion mechanism and the base-catalyzed hydration mechanism, while the latter dominates in aqueous systems. The transformation of the reaction mechanism may relate to the sterically hindered effect of AMP and suggest water plays a significant role in the reaction between CO_2 and AMP. Meanwhile, the detailed

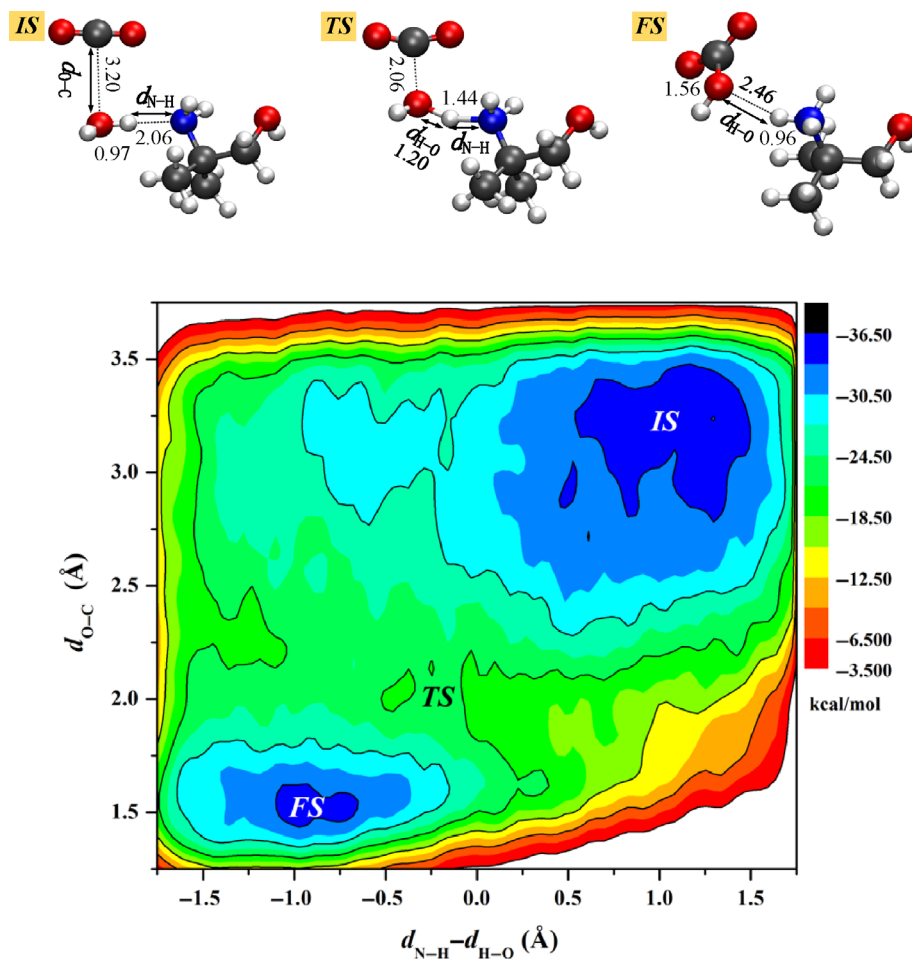


FIGURE 9 Free-energy surface for the bicarbonate (HCO_3^-) formation in aqueous AMP solutions, that is, $\text{AMP} + \text{CO}_2 \rightarrow \text{AMPH}^+ + \text{HCO}_3^-$, predicted from metadynamics-biased Car–Parrinello MD simulation at 313 K. The structures and positions of the initial (IS), transition (TS) and final (FS) states in aqueous AMP solutions are also indicated, where the blue, gray, red and white balls represent the N, C, O, and H atoms, respectively

impact of water on the reaction mechanism and the exact point of the reaction mechanism transformation needs further exploration.

To determine whether the kinetic model is consistent with the fundamental mechanisms of CO_2 absorption in aqueous/nonaqueous solutions or not, we performed *ab initio* molecular dynamics simulations coupled with metadynamics sampling to predict the energy barriers of key elementary reactions.

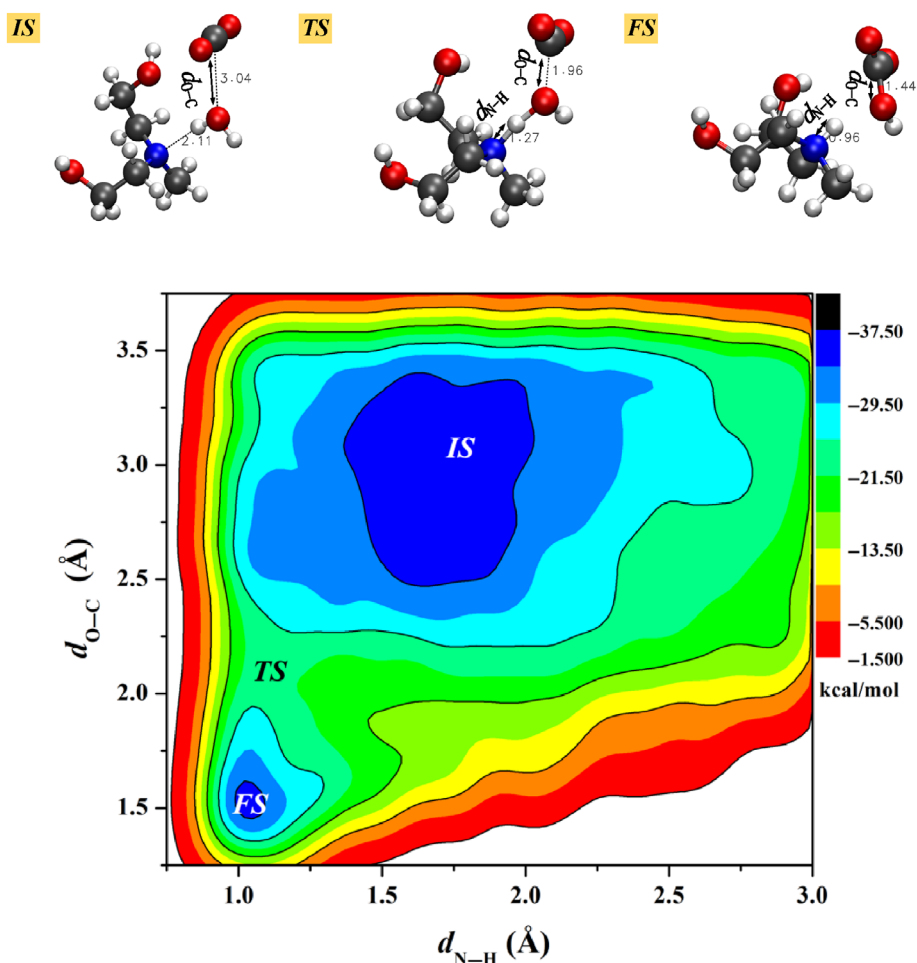
We first estimated the energy barrier of the MEA-zwitterion formation reaction in both nonaqueous and aqueous simulation systems. For the aqueous MEA system, 36 H_2O , 1 MEA, and 1 CO_2 were placed in a cubic periodic box with the side length of 10.78 Å corresponding to about 8.6 wt% aqueous MEA solution; for the nonaqueous MEA simulation system, 15 ethanol, 1 MEA, and 1 CO_2 were placed with the side length of 12.0 Å, corresponding to the nonaqueous MEA solution with the MEA mass concentration of around 8.1 wt%. As illustrated in Figure 8A, in the aqueous MEA solution, at the initial state where the N atom of MEA forms a hydrogen bond with H atom in neighboring H_2O , our simulations predicted $d_{\text{N-C}} = 2.8$ Å and $d_{\text{N-H}} = 2.0$ Å. At the transition state, $d_{\text{N-C}}$ decreased to 1.9 Å while $d_{\text{N-H}}$ increased to 3.0 Å (indicating the broken hydrogen bond between H_2O and MEA). And the $d_{\text{N-C}}$ further decreased to 1.6 Å at the final state, demonstrating the formation of the N–C bond.

First, we calculated the energy barrier for MEA-zwitterion in aqueous solution (water as solvate) to verify the reliability of our

simulations. The energy barrier was predicted to be 7.54 kcal/mol, which is very close to the energy barrier calculated by Yoon et al.⁴² (7.9 kcal/mol) and by Kim et al.⁵¹ (7.67 kcal/mol). Thereafter, the energy barrier for the MEA-zwitterion formation in nonaqueous (ethanol as solvate) was also predicted to be 5.77 kcal/mol, as shown in Figure 8. The relatively high energy barrier in aqueous MEA solutions may suggest that the zwitterion formation in nonaqueous solutions is more kinetic favorable than that in aqueous solutions, which is due to the relatively weak hydrogen bonding in ethanol solutions.⁵² The energy barrier can inflect the reaction rate of the elementary reaction at some exact, while the lower energy barrier for MEA-zwitterion formation in nonaqueous MEA solutions lead to the higher reaction constant in nonaqueous systems ($k_{2,\text{MEA,non}} > k_{2,\text{MEA,aq}}$). Therefore, our simulation results were in well agreement with our experimental results, that the $K_{\text{MEA-MEA,non}}^Z$ (3725.3 1/s/(mol/L)²) was higher than the $K_{\text{MEA-MEA,non}}^Z$ (1916.4 1/s/(mol/L)²) estimated from our kinetic model, as shown in Figure 7A.

To assess the mechanism and the factors that affect the reaction between CO_2 and AMP in aqueous solutions, we calculated the energy barrier of direct HCO_3^- formation through base-catalyzed hydration mechanism in aqueous AMP solution, taking that in aqueous MDEA solution as a reference. The systems contained 38 H_2O , 2 AMP (MDEA), and 1 CO_2 in a cubic periodic box with the side

FIGURE 10 Free-energy surface for bicarbonate (HCO_3^-) formation in aqueous MDEA solutions, that is, $\text{MDEA} + \text{CO}_2 \rightarrow \text{MDEAH}^+ + \text{HCO}_3^-$, predicted from metadynamics-biased Car–Parrinello MD simulation at 313 K. The two collective variables employed were the distance between the H atom of H_2O and the N atom of MDEA ($d_{\text{N-H}}$) and the distance of between the O atom of H_2O and the C atom of CO_2 ($d_{\text{O-C}}$). The structures and positions of the initial (IS), transition (TS) and final (FS) states in aqueous MDEA solutions are also indicated, where the blue, gray, red, and white balls represent the N, C, O, and H atoms, respectively



length of 11.47 Å (11.66 Å). Two collective variables were employed in the simulations: (1) the distance between C of CO_2 and O in the neighboring H_2O , mimicking nucleophilic attack responsible for HCO_3^- formation, (2) the difference of the distance between N of AMP and H in the neighboring H_2O and the distance between H and O in the neighboring H_2O , mimicking the protonation of AMP.

As shown in Figure 9, the protonation of AMP and the HCO_3^- formation may occur simultaneously. The predicted FE barrier for the HCO_3^- formation through the base-catalyzed hydration mechanism in aqueous AMP solutions, was 10.3 kcal/mol, which is very close to the 9.6 kcal/mol calculated by Yoon et al.⁴² and Yamada et al.,²¹ and also compatible to the 8.1 kcal/mol calculated by Stowe et al.³⁹ The energy barrier in aqueous AMP solution (10.3 kcal/mol) is predicted to be higher than that in aqueous MEA solution (7.54 kcal/mol), which agrees well with the higher activation energy of CO_2 absorption in aqueous AMP solution (10.31 kcal/mol from Saha et al.⁵³) than that in aqueous MEA solution (9.56 kcal/mol from Leder⁵⁴) predicted by experiments. Together, our results confirm the reliability and accuracy of our simulations.

Compared to the energy barrier for the formation of AMP-zwitterion in aqueous systems, estimated in the literature (11.7 kcal/mol),⁴² the predicted energy barrier for the HCO_3^- formation was slightly lower. It should be pointed out that in aqueous AMP solutions the base-catalyzed hydration of CO_2 is more kinetic favorable than

the zwitterion formation, which can be explained by the fact that the steric effect of AMP dominates the reaction by affecting the nucleophilicity of N atom⁵⁵, suppressing the thermal rearrangement of adjacent H_2O molecules.³⁹ Considering the thermal instability of AMP-zwitterion at the same time, our simulation results clearly show that the base-catalyzed hydration of CO_2 play a dominant role in the aqueous AMP solutions.

Therefore, our simulation results also verified our experimental results as discussed earlier, indicating that the reaction mechanisms of CO_2 absorption in nonaqueous AMP solutions and aqueous AMP solution were different and that their kinetic model can be described by the linear relationship and the second-order polynomial relationship of k_0 and the AMP concentration, respectively.

Our CPMD-metadynamics simulations estimated the free energy (FE) barrier of the base-catalyzed hydration of CO_2 in aqueous MDEA solutions to be 14.20 kcal/mol; the corresponding FE surface for the reaction was also illustrated in Figure 10. The higher energy barrier in aqueous MDEA solutions than that in aqueous AMP solutions was consistent with the lower reaction constant in aqueous MDEA solutions ($K_{\text{AMP,aq}}^{\text{C}} = 314.41/\text{s}$, $K_{\text{MDEA,aq}}^{\text{C}} = 5.6461/\text{s}$) calculated from the above kinetic model (as shown in Figure 7). It also shows the accuracy of our hypothesis kinetic model described earlier.

5 | CONCLUSIONS

The kinetics of CO₂ absorption in nonaqueous MEA, AMP, MEA + AMP, MEA + MDEA, and aqueous MEA, AMP, MDEA solutions were analyzed in the stopped-flow reactor to understand the fundamental mechanism of the reaction between CO₂ and AMP in both nonaqueous and aqueous solutions. A hypothesis model for the nonaqueous MEA, AMP, MEA + AMP, MEA + MDEA solutions and the aqueous MEA, AMP, MDEA solutions, correlating the measured first-order reaction rate constant to MEA, AMP, MDEA concentration based on the zwitterion mechanism and base-catalyzed hydration mechanism, was verified to be accurately predicting the experimental data.

The reaction kinetics of CO₂ absorption in nonaqueous MEA, nonaqueous MEA + AMP and nonaqueous MEA + MDEA solutions showed that the concentration of AMP or MDEA led to a positive effect on the measured k_0 . These effects are related to the reaction mechanisms, in which the two elementary reactions (the zwitterion formation and proton release of zwitterion) are rate controlling processes, while the AMP and the MDEA take important parts in the later process. The experimental results also demonstrated the different reaction kinetics for CO₂ absorption in nonaqueous AMP and aqueous AMP solutions, owing to the change of dominated reaction issued by the steric hindered effect on the hydrogen bonding and the rearrangement of neighboring molecules.

The FE barriers for key elementary reactions in CO₂ absorption using nonaqueous and aqueous amine solutions were predicted by AIMD metadynamics simulations. Our simulation results showed that the FE barrier for the MEA-zwitterion formation in nonaqueous MEA was lower than that in aqueous MEA, while the FE barrier for the base-catalyzed hydration of CO₂ in aqueous AMP was lower than that in aqueous MDEA. Moreover, compared to the energy barrier for the AMP-zwitterion formation in the aqueous AMP, the lower FE barrier of HCO₃[−] formation indicated that the base-catalyzed hydration of CO₂ was more kinetic favorable. All those simulation results were consistent with the experimental results and verified our kinetic model.

AUTHOR CONTRIBUTIONS

Qinlan Luo: Conceptualization (lead); visualization (lead); writing – original draft (lead). **Rui Dong:** Formal analysis (equal); investigation (lead). **Bohak Yoon:** Software (lead); writing – review and editing (supporting). **Hongxia Gao:** Project administration (lead); writing – original draft (supporting). **Mengjie Chen:** Data curation (equal); investigation (equal). **Gyeong S. Hwang:** Resources (equal); supervision (equal). **Zhiwu Liang:** Project administration (equal); resources (equal); supervision (equal).

DATA AVAILABILITY STATEMENT

Research data are not shared.

ORCID

Zhiwu Liang  <https://orcid.org/0000-0003-1935-0759>

REFERENCES

- Liang Z, Rongwong W, Liu H, et al. Recent progress and new developments in post-combustion carbon-capture technology with amine based solvents. *Int J Greenh Gas Control*. 2015;40:26-54. doi:10.1016/j.ijggc.2015.06.017
- Kenarsari SD, Yang D, Jiang G, et al. Review of recent advances in carbon dioxide separation and capture. *RSC Adv*. 2013;3(45):22739-22773. doi:10.1039/c3ra43965h
- Li J-R, Ma Y, McCarthy MC, et al. Carbon dioxide capture-related gas adsorption and separation in metal-organic frameworks. *Coord Chem Rev*. 2011;255(15–16):1791-1823.
- Tollefson J. Clock ticking on climate action. *Nature*. 2018;562(7726):172-173. doi:10.1038/d41586-018-06876-2
- Vinoba M, Bhagiyalakshmi M, Alqaheem Y, Alomair AA, Pérez A, Rana MS. Recent progress of fillers in mixed matrix membranes for CO₂ separation: a review. *Sep Purif Technol*. 2017;188:431-450. doi:10.1016/j.seppur.2017.07.051
- Theo WL, Lim JS, Hashim H, Mustafa AA, Ho WS. Review of pre-combustion capture and ionic liquid in carbon capture and storage. *Appl Energy*. 2016;183:1633-1663. doi:10.1016/j.apenergy.2016.09.103
- Zheng W, Luo Q, Liu S, et al. New method of kinetic modeling for CO₂ absorption into blended amine systems: a case of MEA/EAE/3DEA1P tri-solvent blends. *AIChE J*. 2022:e17628. doi:10.1002/aic.17628
- Luo Q, Feng B, Liu Z, Zhou Q, Zhang Y, Li N. Experimental study on simultaneous absorption and desorption of CO₂, SO₂, and NO_x using aqueous n-methyldiethanolamine and dimethyl sulfoxide solutions. *Energy Fuel*. 2018;32(3):3647-3659. doi:10.1021/acs.energyfuels.7b03648
- Jiang WS, Luo X, Gao HX, et al. A comparative kinetics study of CO₂ absorption into aqueous DEEA/MEA and DMEA/MEA blended solutions. *Aiche J*. 2018;64(4):1350-1358. doi:10.1002/aic.16024
- Rochelle GT. Amine scrubbing for CO₂ capture. *Science*. 2009;325(5948):1652-1654.
- Nath D, Henni A. Kinetics of carbon dioxide (CO₂) with 3-(dimethylamino)-1-propylamine in water and methanol systems using the stopped-flow technique. *Ind Eng Chem Res*. 2020;59(33):14625-14635. doi:10.1021/acs.iecr.0c01157
- Rayer AV, Mobley PD, Soukri M, et al. Absorption rates of carbon dioxide in amines in hydrophilic and hydrophobic solvents. *Chem Eng J*. 2018;348:514-525. doi:10.1016/j.cej.2018.03.193
- Luo Q, Cao Y, Liu Z, Feng B, Zhou Q, Li N. A feasible process for removal and utilization of CO₂ in thermal power plants by MDEA + DMSO scrubbing and Cu/TiO₂ photocatalytic reduction. *Appl Therm Eng*. 2019;153:369-378. doi:10.1016/j.applthermaleng.2019.02.049
- Ma D, Zhu C, Fu T, Yuan X, Ma Y. An effective hybrid solvent of MEA/DEEA for CO₂ absorption and its mass transfer performance in microreactor. *Sep Purif Technol*. 2020;242:116795. doi:10.1016/j.seppur.2020.116795
- Vaidya PD, Kenig EY. CO₂-alkanolamine reaction kinetics: a review of recent studies. *Chem Eng Technol*. 2007;30(11):1467-1474. doi:10.1002/ceat.200700268
- Lepaumier H, Picq D, Carrette P-L. New amines for CO₂ capture. I. Mechanisms of amine degradation in the presence of CO₂. *Ind Eng Chem Res*. 2009;48(20):9061-9067. doi:10.1021/ie900472x
- Caplow M. Kinetics of carbamate formation and breakdown. *J Am Chem Soc*. 1968;90(24):6795-6803. doi:10.1021/ja01026a041
- Jakobsen JP, Krane J, Svendsen HF. Liquid-phase composition determination in CO₂-H₂O-alkanolamine systems: an NMR study. *Ind Eng Chem Res*. 2005;44(26):9894-9903. doi:10.1021/ie048813
- Alper E. Reaction mechanism and kinetics of aqueous solutions of 2-amino-2-methyl-1-propanol and carbon dioxide. *Ind Eng Chem Res*. 1990;29(8):1725-1728. doi:10.1021/ie00104a023
- Yih SM, Shen KP. Kinetics of carbon dioxide reaction with sterically hindered 2-amino-2-methyl-1-propanol aqueous solutions. *Ind Eng Chem Res*. 1988;27(12):2237-2241. doi:10.1021/ie00084a008

21. Yamada H, Matsuzaki Y, Higashii T, Kazama S. Density functional theory study on carbon dioxide absorption into aqueous solutions of 2-amino-2-methyl-1-propanol using a continuum solvation model. *J Phys Chem A*. 2011;115(14):3079-3086. doi:[10.1021/jp109851k](https://doi.org/10.1021/jp109851k)
22. Xie H-B, He N, Song Z, Chen J, Li X. Theoretical investigation on the different reaction mechanisms of aqueous 2-Amino-2-methyl-1-propanol and monoethanolamine with CO₂. *Ind Eng Chem Res*. 2014;53(8):3363-3372. doi:[10.1021/ie403280h](https://doi.org/10.1021/ie403280h)
23. Mobley PD, Rayer AV, Tanthana J, et al. CO₂ capture using fluorinated hydrophobic solvents. *Ind Eng Chem Res*. 2017;56(41):11958-11966. doi:[10.1021/acs.iecr.7b03088](https://doi.org/10.1021/acs.iecr.7b03088)
24. Zheng X, Qu D, Zhang F, Liu Y, Qin G. Measurements and calculations of thermal conductivity for liquid n-octane and n-decane. *Fluid Phase Equilib*. 2021;533:112940. doi:[10.1016/j.fluid.2021.112940](https://doi.org/10.1016/j.fluid.2021.112940)
25. Wang Y, Dong Y, Zhang L, et al. Carbon dioxide capture by non-aqueous blend in rotating packed bed reactor: absorption and desorption investigation. *Sep Purif Technol*. 2021;269:118714.
26. Patil MP, Vaidya PD. Aqueous mixtures of AMP, HMDA-N,N'-dimethyl and TEG for CO₂ separation: a study on equilibrium and reaction kinetics. *Chem Eng Commun*. 2020;207(10):1440-1450. doi:[10.1080/00986445.2019.1657419](https://doi.org/10.1080/00986445.2019.1657419)
27. Zhan X, Lv B, Yang K, Jing G, Zhou Z. Dual-functionalized ionic liquid biphasic solvent for carbon dioxide capture: high-efficiency and energy saving. *Environ Sci Technol*. 2020;54(10):6281-6288. doi:[10.1021/acs.est.0c00335](https://doi.org/10.1021/acs.est.0c00335)
28. Kadiwala S, Rayer AV, Henni A. Kinetics of carbon dioxide (CO₂) with ethylenediamine, 3-amino-1-propanol in methanol and ethanol, and with 1-dimethylamino-2-propanol and 3-dimethylamino-1-propanol in water using stopped-flow technique. *Chem Eng J*. 2012;179:262-271. doi:[10.1016/j.cej.2011.10.093](https://doi.org/10.1016/j.cej.2011.10.093)
29. Liu H, Liang Z, Sema T, et al. Kinetics of CO₂ absorption into a novel 1-diethylamino-2-propanol solvent using stopped-flow technique. *AIChE J*. 2014;60(10):3502-3510. doi:[10.1002/aic.14532](https://doi.org/10.1002/aic.14532)
30. Duatete FPG, Orhan OY, Alper E. Kinetics of carbon dioxide absorption by nonaqueous solutions of promoted sterically hindered amines. *Energy Procedia*. 2017;114:57-65. doi:[10.1016/j.egypro.2017.03.1147](https://doi.org/10.1016/j.egypro.2017.03.1147)
31. Ali SH, Merchant SQ, Fahim MA. Reaction kinetics of some secondary alkanolamines with carbon dioxide in aqueous solutions by stopped flow technique. *Sep Purif Technol*. 2002;27(2):121-136. doi:[10.1016/S1383-5866\(01\)00206-4](https://doi.org/10.1016/S1383-5866(01)00206-4)
32. Conway W, Wang X, Fernandes D, et al. Toward the understanding of chemical absorption processes for post-combustion capture of carbon dioxide: electronic and steric considerations from the kinetics of reactions of CO₂(aq) with sterically hindered amines. *Environ Sci Technol*. 2013;47(2):1163-1169. doi:[10.1021/es3025885](https://doi.org/10.1021/es3025885)
33. Liu B, Luo X, Gao H, et al. Reaction kinetics of the absorption of carbon dioxide (CO₂) in aqueous solutions of sterically hindered secondary alkanolamines using the stopped-flow technique. *Chem Eng Sci*. 2017;170:16-25. doi:[10.1016/j.ces.2017.02.044](https://doi.org/10.1016/j.ces.2017.02.044)
34. Liu S, Ling H, Gao H, Tontiwachwuthikul P, Liang Z, Zhang H. Kinetics and new Brønsted correlations study of CO₂ absorption into primary and secondary alkanolamine with and without steric-hindrance. *Sep Purif Technol*. 2020;233:115998. doi:[10.1016/j.seppur.2019.115998](https://doi.org/10.1016/j.seppur.2019.115998)
35. Bougie F, Illiuta MC. Sterically hindered amine-based absorbents for the removal of CO₂ from gas streams. *J Chem Eng Data*. 2012;57(3):635-669. doi:[10.1021/je200731v](https://doi.org/10.1021/je200731v)
36. Liu S, Gao H, Luo X, Liang Z. Kinetics and new mechanism study of CO₂ absorption into water and tertiary amine solutions by stopped-flow technique. *AIChE J*. 2019;65(2):652-661. doi:[10.1002/aic.16469](https://doi.org/10.1002/aic.16469)
37. Ali SH. Kinetics of the reaction of carbon dioxide with blends of amines in aqueous media using the stopped-flow technique. *Int J Chem Kinet*. 2005;37(7):391-405. doi:[10.1002/kin.20059](https://doi.org/10.1002/kin.20059)
38. Zhang Y, Yang W. Comment on "generalized gradient approximation made simple". *Phys Rev Lett*. 1998;80(4):890. doi:[10.1103/PhysRevLett.80.890](https://doi.org/10.1103/PhysRevLett.80.890)
39. Stowe HM, Hwang GS. Molecular insights into the enhanced rate of CO₂ absorption to produce bicarbonate in aqueous 2-amino-2-methyl-1-propanol. *Phys Chem Chem Phys*. 2017;19(47):32116-32124. doi:[10.1039/C7CP05580C](https://doi.org/10.1039/C7CP05580C)
40. Stowe HM, Paek E, Hwang GS. First-principles assessment of CO₂ capture mechanisms in aqueous piperazine solution. *Phys Chem Chem Phys*. 2016;18(36):25296-25307. doi:[10.1039/C6CP03584A](https://doi.org/10.1039/C6CP03584A)
41. Mushrif SH, Varghese JJ, Krishnamurthy CB. Solvation dynamics and energetics of intramolecular hydride transfer reactions in biomass conversion. *Phys Chem Chem Phys*. 2015;17(7):4961-4969. doi:[10.1039/C4CP05063K](https://doi.org/10.1039/C4CP05063K)
42. Yoon B, Hwang GS. Anomalous facile carbamate formation at high stripping temperatures from carbon dioxide reaction with 2-Amino-2-methyl-1-propanol in aqueous solution. *ACS Sustain Chem Eng*. 2020;8(50):18671-18677. doi:[10.1021/acssuschemeng.0c07203](https://doi.org/10.1021/acssuschemeng.0c07203)
43. Yoon B, Stowe HM, Hwang GS. Molecular mechanisms for thermal degradation of CO₂-loaded aqueous monoethanolamine solution: a first-principles study. *Phys Chem Chem Phys*. 2019;21(39):22132-22139.
44. Crooks JE, Donnellan JP. Kinetics of the reaction between carbon dioxide and tertiary amines. *J Org Chem*. 1990;55(4):1372-1374. doi:[10.1021/jo00291a056](https://doi.org/10.1021/jo00291a056)
45. Donaldson TL, Nguyen YN. Carbon dioxide reaction kinetics and transport in aqueous amine membranes. *Ind Eng Chem Fundam*. 1980;19(3):260-266. doi:[10.1021/i160075a005](https://doi.org/10.1021/i160075a005)
46. Chakraborty AK, Astarita G, Bischoff KB. CO₂ absorption in aqueous solutions of hindered amines. *Chem Eng Sci*. 1986;41(4):997-1003. doi:[10.1016/0009-2509\(86\)87185-8](https://doi.org/10.1016/0009-2509(86)87185-8)
47. Camacho F, Sánchez S, Pacheco R, Sánchez A, La Rubia MD. Thermal effects of CO₂ absorption in aqueous solutions of 2-amino-2-methyl-1-propanol. *AIChE J*. 2005;51(10):2769-2777. doi:[10.1002/aic.10523](https://doi.org/10.1002/aic.10523)
48. Henni A, Li J, Tontiwachwuthikul P. Reaction kinetics of CO₂ in aqueous 1-amino-2-propanol, 3-amino-1-propanol, and dimethyl-monoethanolamine solutions in the temperature range of 298–313 K using the stopped-flow technique. *Ind Eng Chem Res*. 2008;47(7):2213-2220. doi:[10.1021/ie070587r](https://doi.org/10.1021/ie070587r)
49. Versteeg GF, van Swaaij WPM. On the kinetics between CO₂ and alkanolamines both in aqueous and non-aqueous solutions—II. Tertiary amines. *Chem Eng Sci*. 1988;43(3):587-591. doi:[10.1016/0009-2509\(88\)87018-0](https://doi.org/10.1016/0009-2509(88)87018-0)
50. Littel R, Bos M, Knoop GJ. Dissociation constants of some alkanolamines at 293, 303, 318, and 333 K. *J Chem Eng Data*. 1990;35:276-277. doi:[10.1021/je00061a014](https://doi.org/10.1021/je00061a014)
51. Kim S, Shi H, Lee JY. CO₂ absorption mechanism in amine solvents and enhancement of CO₂ capture capability in blended amine solvent. *Int J Greenh Gas Control*. 2016;45:181-188. doi:[10.1016/j.jggc.2015.12.024](https://doi.org/10.1016/j.jggc.2015.12.024)
52. Zheng X, Bao Y, Qu D, Liu Y, Qin G. Measurement and modeling of thermal conductivity for short chain methyl esters: methyl butyrate and methyl caproate. *J Chem Thermodyn*. 2021;159:106486. doi:[10.1016/j.jct.2021.106486](https://doi.org/10.1016/j.jct.2021.106486)
53. Saha AK, Bandyopadhyay SS, Biswas AK. Kinetics of absorption of CO₂ into aqueous solutions of 2-amino-2-methyl-1-propanol. *Chem Eng Sci*. 1995;50(22):3587-3598. doi:[10.1016/0009-2509\(95\)00187-A](https://doi.org/10.1016/0009-2509(95)00187-A)
54. Leder F. The absorption of CO₂ into chemically reactive solutions at high temperatures. *Chem Eng Sci*. 1971;26(9):1381-1390. doi:[10.1016/0009-2509\(71\)80058-1](https://doi.org/10.1016/0009-2509(71)80058-1)
55. Huang KH, Wei Z, Cooks RG. Accelerated reactions of amines with carbon dioxide driven by superacid at the microdroplet interface. *Chem Sci*. 2020;12(6):2242-2250.

How to cite this article: Luo Q, Dong R, Yoon B, et al. An experimental/computational study of steric hindrance effects on CO₂ absorption in (non)aqueous amine solutions. *AIChE J*. 2022;68(7):e17701. doi:[10.1002/aic.17701](https://doi.org/10.1002/aic.17701)